Established in 1871

Swiss Medical Weekly

Formerly: Schweizerische Medizinische Wochenschrift

An open access, online journal • www.smw.ch

Review article: Biomedical intelligence | Published 6 August 2016, doi:10.4414/smw.2016.14328

Cite this as: Swiss Med Wkly. 2016;146:w14328

Dual-energy computed tomographic imaging of pulmonary hypertension

Anne-Lise Hachulla[a,b], Frédéric Lador[b,c,d], Paola M. Soccal[b,c,d], Xavier Montet[a,b,d], Maurice Beghetti[b,d,e]

[a] Division of Radiology, University Hospitals of Geneva, Switzerland

[b] Pulmonary Hypertension Programme, University Hospitals of Geneva, Switzerland

[c] Division of Pneumology, University Hospitals of Geneva, Switzerland

[d] Geneva University, Faculty of Medicine

[e] Paediatric Cardiology Unit, Children's University Hospital, Geneva, Switzerland

Summary

Dual-energy computed tomography (DECT) angiography of the chest provides a combined morphological and functional analysis of the lung, usually obtained in a single acquisition without extra radiation or injection of extra intravenous iodine contrast.

The parenchymal iodine maps generated by DECT are well correlated with scintigraphy, and are becoming an essential tool for evaluating patients with pulmonary vascular diseases.

With a single DECT acquisition, complete imaging of pulmonary hypertension is now available, displaying vascular anatomy, parenchymal morphology and functional assessment. Triangular pulmonary perfusion defects in chronic thromboembolic pulmonary hypertension may be clearly analysed even in the presence of distal arterial occlusion. Perfusion heterogeneities seen in patients with pulmonary arterial hypertension reflect mosaic perfusion and may be helpful for the diagnosis, severity assessment and prognosis of the disease. Vascular or parenchymal abnormalities can also be analysed with perfusion defects to determine their aetiology. Pulmonary arterial hypertension due to congenital heart disease can be assessed with a single DECT, even in the neonatal population. Furthermore, new applications are emerging with ventilation imaging or myocardial perfusion imaging obtained by DECT and should be considered.

In conclusion, DECT of the thorax enables the simultaneous and noninvasive assessment of vascular anatomy, parenchymal morphology and functional pulmonary imaging in various groups of PH.

Key words: *pulmonary hypertension; noninvasive imaging; dual-energy CT; imaging; emerging technologies; chronic thromboembolic pulmonary hypertension; pulmonary arterial hypertension; PH due to chronic lung diseases; PH due to left heart disease*

Introduction

Pulmonary hypertension (PH) is a haemodynamic and pathophysiological condition defined as an increase in mean pulmonary arterial pressure (mPAP) above or equal to 25 mm Hg at rest as assessed with right heart catheterisation [1]. Because multiple clinical conditions are involved, five different aetiological groups are defined according to their specific and various pathological characteristics [2].

Regarding the severe prognosis of PH, the first major challenge remains early diagnosis, because of its insidious symptoms; in fact, data show that most patients present a severe haemodynamic alteration associated with delayed diagnosis [3, 4]. The second issue is to determine the PH group in order to decide upon an optimal treatment. The distinction between pulmonary arterial hypertension (PAH) and other causes of PH [5], even in the paediatric PH population [6], may be challenging.

Conventional computed tomography (CT) of the chest may be helpful in diagnosing PH and determining underlying pathologies such as pulmonary or vascular abnormalities. Furthermore, functional information can then be added to CT by the use of a dual-energy protocol. As a consequence, new and noninvasive tools that might increase diagnostic accuracy and functional imaging [7–11] are being developed. Magnetic resonance imaging offers functional quantification but suffers from a lack of resolution of lung parenchyma and pulmonary arteries [12].

Dual-energy computed tomography (DECT) holds promise by combining morphological analysis with functional information on pulmonary perfusion. In this review, we describe how DECT imaging with perfusion maps may play an important role in the complete imaging of PH [13, 14].

DECT technology and principles

DECT is a recently available technology that enables combined functional and morphological analysis of the lung. Several DECT techniques have been proposed [15], including dual-source systems with two X-ray tubes for simul-

taneous low- and high-kilovoltage image acquisition [16]. Another technique uses rapid kilovoltage switching at low- and high-kilovoltage spectra with a single-source CT system [17]. Whatever the technique used, DECT images are obtained in a single simple acquisition.

Because of the attenuation properties of iodine at two different photon energies (80 and 140 kV), a dual-energy technique can generate pulmonary blood volume maps and quantify the iodine concentration in the parenchyma. It has been demonstrated that the local distribution of iodine contrast medium correlates well with pulmonary perfusion [18]. The generated pulmonary blood volume maps are combined with mediastinal images to permit simultaneous analysis of the grey-scale vasculature and colour-scale parenchymal perfusion, with parenchymal images (fig. 1). Furthermore, the iodine concentration in the lung allows an objective and quantitative analysis.

In comparison with conventional CT, no additional intravenous iodine contrast medium is needed; functional image processing is simply added. Furthermore, it is not associated with increased radiation levels because the radiation dose is split between the two tubes [19]. Table 1 summarises the mean effective dose reported in literature of non-invasive or invasive examinations used in PH imaging [18, 20–22]. In our centre, the mean dose-length-product for a DECT protocol is 252 ± 92 mGy.cm, corresponding to a mean effective dose of 3.5 ± 1.3 mSv.

To date, published works show that perfusion measured with DECT has an excellent correlation with the perfusion measured with pulmonary scintigraphy. Several studies have already demonstrated that the perfusion maps can be used to assess qualitatively and quantitatively areas of lung hypoperfusion, in a method similar to scintigraphy [23, 24]. Furthermore, DECT enables "superior anatomic and functional comprehension" by simultaneously recording the vascular anatomy, parenchymal morphology and functional perfusion without extra radiation dosage. DECT seems to offer clear advantages in comparison with conventional CT or pulmonary scintigraphy (table 2).

Many applications are available for clinical use, and perfusion maps are well established for evaluating acute pulmonary embolism [25–28]. In fact, with DECT it is possible to colour code iodine distribution in the lung parenchyma, in order to visualise and quantify perfusion defects caused by emboli. These perfusion defects reflect the physiological impairment caused by embolic disease, and are correlated with endoluminal clot burden and increased right-to-left ventricular ratios [21, 29, 30], or with the prognosis of pulmonary embolism [31].

Nevertheless, these iodine maps require careful interpretation. Pseudodefects can be pitfalls, because of artefacts such as beam-hardening artefacts or motion artefacts near to the heart or diaphragm. These artefacts need to be avoided or recognised before a diagnosis is reached [32]. Iodine maps always require interpretation in relation to morphological pulmonary reconstructions, in order to avoid misdiagnosis of true segmental perfusion defects due to pulmonary pathologies such as emphysema or bronchopathies, Finally, because of the field of view, greater noise and a pitch below 3, the DECT protocol has some limitations for obese patients (body mass index >30 kg/m^2), or patients with severe tachypnoea, where an enlarged field of view or a higher pitch would be more appropriate."

DECT in chronic thromboembolic pulmonary hypertension (group 4)

Similar segmental perfusion defects in patients with chronic thromboembolic pulmonary hypertension (CTEPH) have already been widely evaluated [33–37], as previously studied in acute pulmonary embolism. The incomplete resolution of endovascular thromboembolic material is responsible for intravascular scars, resulting in stenosis, web formation or occlusion of pulmonary arteries. The resulting perfusion heterogeneities are well described on planar scintigraphy and, more recently, DECT imaging. These segmental perfusion defects are readily recognised as triangular areas following the pulmonary arterial tree. In fact, the triangular defects are seen more frequently in segments with

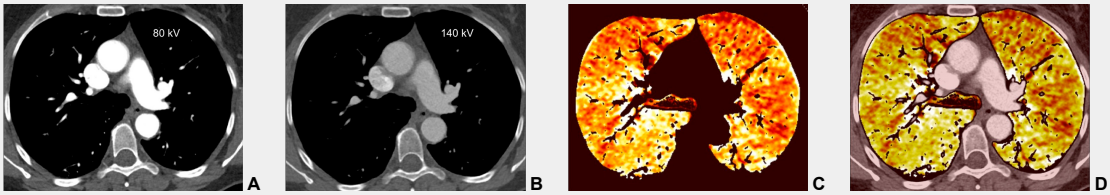

Figure 1

Technical principles. The dual-energy system with two X-ray tubes permits simultaneous 80 (**A**) and 140 kV (**B**) image acquisition in order to generate an iodine map (**C**) fused with mediastinal reconstructions (**D**).

Table 1: Mean effective doses reported in literature of imaging uses applicable to pulmonary hypertension.

	Postero-anterior and lateral chest X-ray	Conventional chest CT	Chest dual-energy CT	Pulmonary angiography	Lung perfusion (99mTc-MAA)	Lung ventilation (xenon 133)	Lung ventilation (99mTc-DTPA)	Right/left heart cardiac catheterisation
Mean effective dose in mSv (range)	0.1 (0.05–0.24)	5.6	3.85 (2.0–5.2)	5 (4.1–9)	2.0	0.5	0.2	7 (2.0–15.8)

CT = computed tomography; DTPA = diethylenetriaminepentaacetic acid; MAA = microaggregated albumin

severe pulmonary arterial features such as webs, bands, stenoses or occlusions [35] (fig. 2). The extent of perfusion defects seen on DECT could be a prognostic indicator for thromboendarterectomy [36]. Thus, DECT can provide a single unique acquisition for diagnosis, planning and follow-up of CTEPH, and correlates well with pulmonary angiography and scintigraphy (fig. 3).

Conventional CT angiography (CTA) can naturally show direct vascular signs of CTEPH or a mosaic lung pattern [38]. Sometimes peripheral subsegmental occlusions may be difficult or poorly visualised, and conventional CTA cannot provide functional information about pulmonary perfusion. For these reasons, single source CTA has a sensitivity of 64–70% for depiction of segmental and subsegmental chronic thromboembolism compared with selective pulmonary angiography [39]. This is why it has been reported that the sensitivity for the diagnosis of CTEPH with conventional CTA is 51% versus 97% with scintigraphy [40]. With DECT, perfusion maps could provide functional information similar to perfusion scintigraphy and also can provide, in a single simple technique, high anatomic resolution of vessels with functional imaging. Furthermore, with a retrospective analysis after the hypoperfusion depiction, it will be possible to diagnose subsegmental signs of CTEPH and increase the sensitivity of the diagnosis.

Several studies assessed the correlation of DECT with scintigraphy. A correlation between DECT and single photon emission computed tomography (SPECT) in 51 patients found that DECT with iodine maps had a sensitivity of 96% and a specificity of 76% for CTEPH [34]. The authors concluded that iodine maps enable depiction of smaller areas of hypoperfusion because of higher spatial resolution and that DECT is comparable to scintigraphy for pulmonary perfusion analysis in CTEPH. The resolution of DECT, scintigraphy and SPECT is 0.5 mm, 7–8 mm and 3–4 mm, respectively. However, intra-arterial defects can be confidently detected only in vessels measuring more than 2 mm. Consequently, it has been reported that perfusion defects are occasionally seen in the absence of a visible embolus on CTA [25, 41]. These small defects may reflect hypoperfusion below the resolution limits of conventional CTA for the visualisation of emboli (fig. 4).

Scintigraphy does not provide morphological information such as parenchymal changes or vascular anatomy and can lead to diagnostic errors, such as acute pulmonary embolism. The integrated DECT approach with lung and vascular analysis combined with functional analysis may, therefore,

Table 2: Comparison between conventional CT, pulmonary scintigraphy and DECT imaging for pulmonary hypertension imaging assessment.

	Conventional CT	**Pulmonary scintigraphy**	**DECT Imaging**
Vascular analysis	Pulmonary artery diameter Pulmonary arteries with diagnosis of clot, stenosis, occlusion, webs, bands Systemic artery analysis Cardiac changes (RV dilatation and hypertrophy)	No morphological vascular analysis	*Identical to conventional CT:* Pulmonary artery diameter Pulmonary arteries with diagnosis of clot, stenosis, occlusion, webs, bands Systemic artery analysis Cardiac changes (RV dilatation and hypertrophy)
Parenchymal analysis	Mosaic lung perfusion Pulmonary infarcts Ground glass nodules	No morphological parenchymal analysis *If ventilation imaging:* Ventilation- perfusion relationship assessed	*Identical to conventional CT:* Mosaic lung perfusion Pulmonary infarcts Ground glass nodules
Perfusion analysis	No perfusion analysis	*Gold standard for perfusion analysis:* Well-defined segmental perfusion defects Or a “mottled” pattern	*Iodine maps correlated with scintigraphy:* Well-defined segmental perfusion defects Or a “mottled” pattern With regional analysis

CT = computed tomography; DECT = dual-energy computed tomography; RV = right ventricle

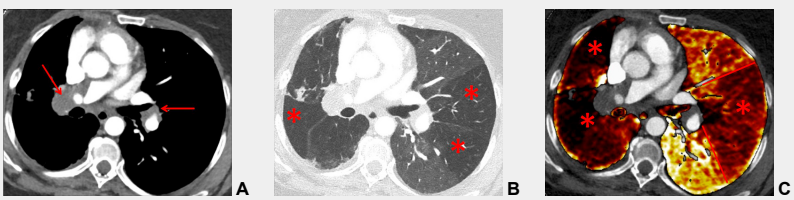

Figure 2

Chronic thromboembolic pulmonary hypertension (CTEPH). Vascular (**A**) and parenchymal (**B**) signs of CTEPH with proximal marginal occlusion (arrows) and mosaic pattern (stars). Functional information simply added with triangular perfusion defects (stars) on the iodine maps (**C**).

be more advantageous than a sequential approach with ventilation/perfusion scintigraphy and conventional CTA. The presence of matched ventilation and perfusion defects can be a confounder in the scintigraphic evaluation and it may be impossible to determine if these areas reflect a chronic physiological response to acute or chronic vascular obstruction or concomitant obstructive airways disease. Thus, perfusion defects seen in DECT always have to be correlated with morphological changes to help determine their significance.

DECT in pulmonary arterial hypertension (group 1) and pulmonary hypertension with unclear multifactorial mechanisms (group 5)

Nowadays, DECT imaging can be used for pathologies other than CTEPH and seems to offer advantages for PH characterisation because different DECT findings have been described in acute pulmonary embolism, CTEPH and idiopathic PAH (IPAH). In fact, perfusion defects are smaller and less defined in PAH than in CTEPH. This is likely due to focal under- and overperfusion as a result of the structural pulmonary vascular changes that occur in PH, which include vascular endothelial damage, cellular proliferation and occlusion in the distal pulmonary vasculature. Perfusion heterogeneities in DECT imaging are also common and seen in most cases of PAH. Findings of perfusion inhomogeneities related PAH have long been recognised in scintigraphy, and often are referred to as having a "mottled" pattern [42]. These perfusion defects are different from those seen in CTEPH, with nonsegmental and poorly defined defects (fig. 5). This heterogeneity is related to the severity of the disease. In PAH, this perfusion variability on scintigraphy is well correlated with pulmonary vascular resistance, as Talwar et al. showed [43]. Recently, similar results were published for DECT techniques (fig. 6). Ameli-Renani et al. described an increased enhancement of pulmonary arteries with reduced iodine lung perfusion in PH, and a good correlation of DECT perfusion heterogeneities with pulmonary vascular resistance; they showed a greater heterogeneity in parenchymal iodine

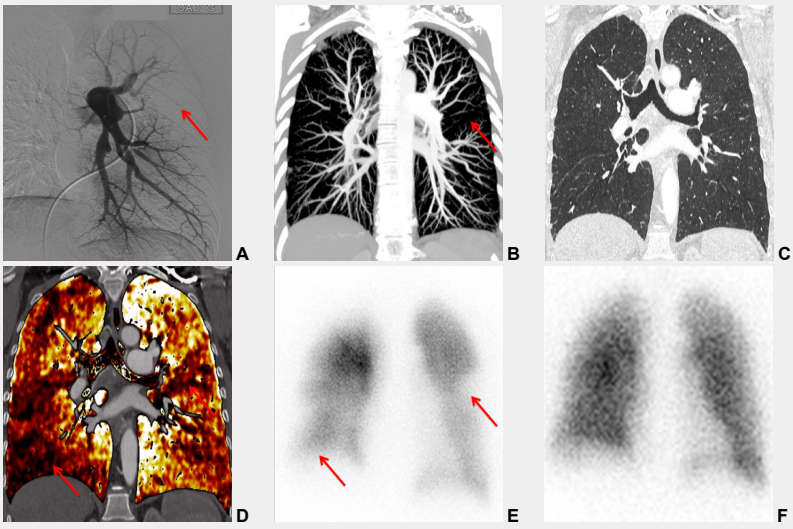

Figure 3

Chronic thromboembolic pulmonary hypertension (CTEPH). Segmental occlusions of pulmonary arteries (arrow) in the pulmonary angiography (**A**) are clearly visible on the CT angiography (**B**), with normal lung (**C**), and responsible for triangular perfusion defects (arrows) on the perfusion maps (**D**) confirmed by the ventilation-perfusion scintigraphy (**E–F**).

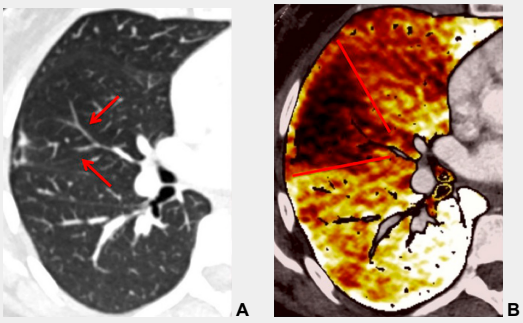

Figure 4

Peripheral chronic thromboembolic pulmonary hypertension (CTEPH). No visible pulmonary artery emboli on standard CTPA are seen (arrows) (**A**) but a wide perfusion defect on the perfusion maps is depicted (**B**) and allows the diagnosis of peripheral CTEPH.

maps in PH without pulmonary embolism [13]. The authors concluded that perfusion heterogeneities seen in DECT appear to be a direct reflection of pulmonary vascular resistance.

Chest DECT seems an increasingly essential tool for imaging pulmonary perfusion, and could be used not only for IPAH but also for all causes in groups 1 and 5, as demonstrated in portopulmonary hypertension (fig. 7). Furthermore, some ground-glass opacities can be visualised in PAH, for example in the case of Eisenmenger's syndrome shown in figure 8. Therefore, iodine maps could help to differentiate ground-glass opacities due to infiltration from those of vascular origin, as has already been reported in the literature [44].

Finally, applications of the DECT protocol are also an emerging technology for investigating congenital heart disease in the adult or paediatric populations. Pulmonary perfusion imaging is available even for very small children with the same DECT acquisition and without extra radiation dosage. This DECT allows combined morphological analysis of the congenital heart disease and functional assessment of pulmonary perfusion in the neonatal population (fig. 9).

DECT in pulmonary hypertension due to lung disease and/or hypoxia (group 3)

DECT simultaneously provides an assessment of the perfusion status of the lungs and parenchymal images in a single acquisition. Because of this simultaneous study of the perfusion maps with conventional parenchymal images, the severity of pulmonary hypoperfusion can be determined. Perfusion abnormalities may be caused by parenchymal destruction as in interstitial lung disease, bronchopathy or pulmonary emphysema, and it is mandatory to analyse the iodine maps with the lung reconstructions before deciding on the origin of perfusion defects. Perfusion defects may match areas of parenchymal destruction. For example, perfusion defects in areas of bronchopathy suggest hypoperfu-

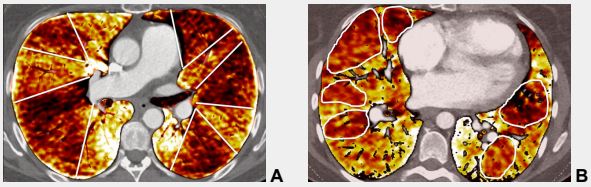

Figure 5

Difference of perfusion defects in pulmonary hypertension depending on the aetiology: triangular well-defined defect seen in chronic thromboembolic pulmonary hypertension (**A**) and poorly defined defect with mottled pattern seen in idiopathic pulmonary arterial hypertension (**B**).

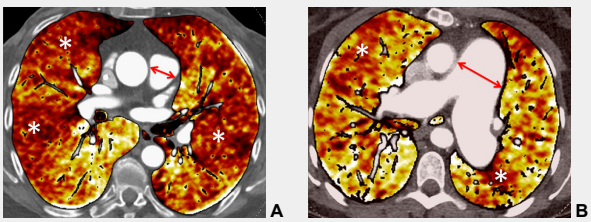

Figure 6

Perfusion heterogeneities in idiopathic pulmonary artery hypertension (stars) in two different patients (**A/B**). The dilatation of the arteries in pulmonary hypertension (arrows) is not always observed depending on the severity of pulmonary hypertension.

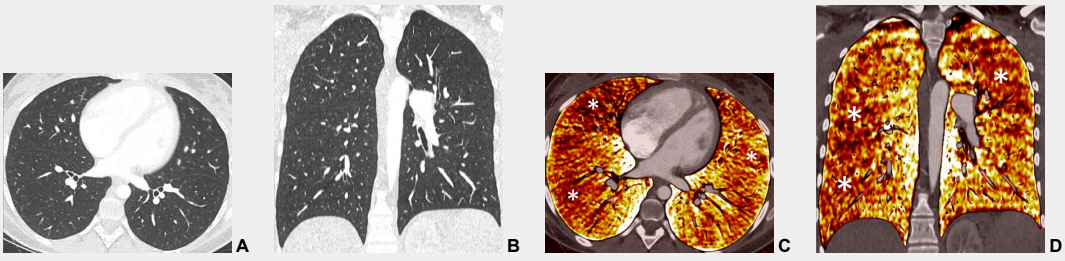

Figure 7

Portopulmonary hypertension in a 16-year-old. No abnormalities were found on morphological computed tomography (**A/B**), but heterogeneous perfusions were present on the perfusion map (stars, **C/D**).

sion due to airways disease secondary to pulmonary artery vasoconstriction (fig. 10).

Perfusion could also be assessed with DECT in patients with PH caused by emphysema or lung fibrosis (fig. 11). The regional severity of pulmonary emphysema can be evaluated by correlating functional perfusion images with anatomical changes. Lee and coworkers found that DECT could be used for emphysema quantification and regional perfusion evaluation by use of iodine maps [45]. In emphysema, destruction of alveoli and interstitial spaces leads to a loss of pulmonary vessels, responsible for a decrease in perfusion. In lung fibrosis, perfusion defects reflect pathological processes such as small-vessel remodelling or fibrotic obliteration of the pulmonary vasculature.

Recently, ventilation imaging with DECT has emerged. Several studies have evaluated regional lung ventilation imaging with DECT after xenon [46–48] or krypton inhalation [49]. Ventilation maps promise to be a supplementary

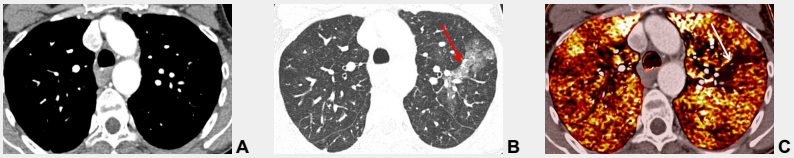

Figure 8

Eisenmenger's syndrome secondary to a large ventricular septal defect. No vascular abnormalities were seen (**A**) but some ground-glass opacities (arrow) (**B**) with the absence of perfusion corresponded to vascular ground-glass opacities surrounded by clear heterogeneous pulmonary perfusion (**C**).

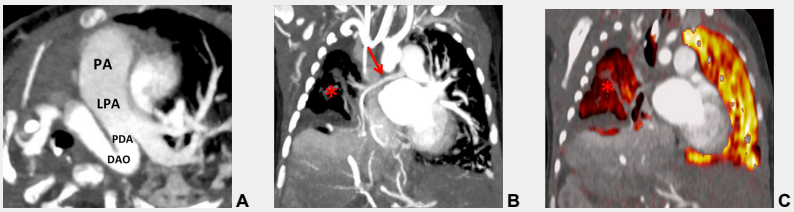

Figure 9

Pulmonary hypertension due to a patent ductus arteriosus (PDA) connecting the descending aorta (DAO) to the left pulmonary artery (LPA) (**A**) in a 2-month-old boy treated for a right diaphragmatic hernia (**B**) resulting in hypoplasia of the right pulmonary artery (arrow). The functional consequences (**C**) are extended hypoperfusion of the right lung (star).

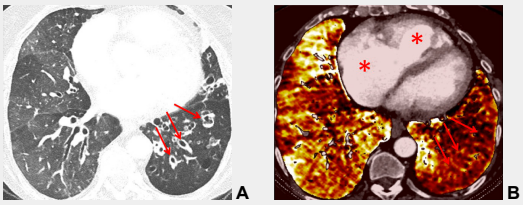

Figure 10

Severe bronchopathy (arrow) in the left lower lobe (**A**) associated with extended hypoperfusion (arrow) and dilatation of the right cardiac cavities (stars) (**B**).

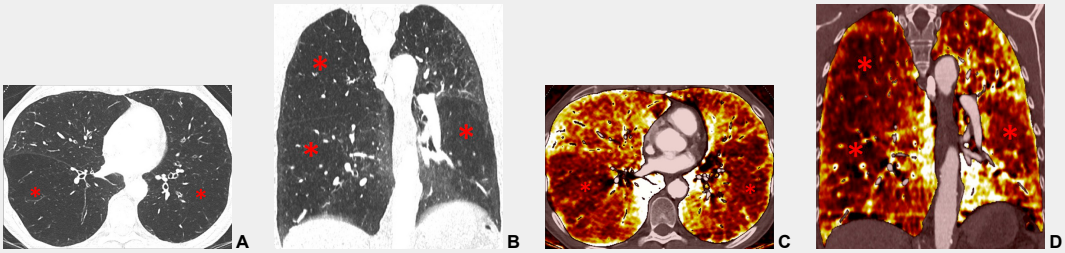

Figure 11

Chronic obstructive pulmonary disease. Correlation between panlobular emphysema (**A/B**) and pulmonary hypoperfusion (**C/D**) (stars).

technique and enable the combined assessment of regional ventilation and perfusion, a surrogate for lung scintigraphy. With xenon- or krypton-enhanced DECT, ventilation maps can be generated to analyse regional ventilation, for example in chronic obstructive pulmonary disease (COPD) or lung fibrosis. This combination of lung perfusion and ventilation mapping promises a complete and comprehensive assessment of ventilation, perfusion and morphology of the pulmonary parenchyma [50].

DECT in pulmonary hypertension due to left heart disease (group 2)

PH due to left heart disease promotes a cascade of damaging anatomical and functional changes of the pulmonary venous, capillary and arterial circulation, eventually accelerating right ventricular dysfunction and failure. Several authors have shown that patients with left heart disease had symmetrical perfusion defects in the lower lungs on pulmonary ventilation/perfusion scintigraphy, which were caused by redistribution of pulmonary blood flow [51].
Clinical cardiac DECT applications are emerging and have been described for dual-energy myocardium perfusion (with or without a stress test) or myocardium viability imaging [52–54]. Cardiac DECT techniques promise to assess simultaneously coronary artery stenosis and functional myocardial perfusion, with exactly the same technology as pulmonary DECT. With a stress test, it will be possible to identify haemodynamically significant coronary stenosis [55]. Furthermore, late enhancement of the myocardium on DECT could identify chronic myocardial infarction and its eventual viability as well as the images obtained using cardiac magnetic resonance imaging [56, 57]. Thus, cardiac DECT should be considered for the depiction of left heart disease in patients with PH.

Conclusion

Because DECT can combine morphological pulmonary vascular imaging and perfusion map characterisation, the technique provides a powerful “one-stop” examination of pulmonary hypertension for diagnosis, assessment of severity or follow-up, irrespective of the cause or age, and with no extra radiation. The role of DECT in the diagnostic algorithm of PH has to be confirmed by further studies.

Acknowledgement: The authors would like to thank Dr Catherine Torriani Hammon and Angela Frei for careful review of the manuscript.
Disclosure statement: No financial support and no other potential conflict of interest relevant to this article was reported.

Correspondence: *Anne-Lise Hachulla, MD, Division of Radiology, Cardio-vascular and Thoracic Imaging Unit, Pulmonary Hypertension Program of Geneva, University Hospitals of Geneva, Rue Gabrielle-Perret-Gentil 4, 1211 Geneva, anne-lise.hachullalemaire[at]hcuge.ch*

References

1 Hoeper MM, Bogaard HJ, Condliffe R, Frantz R, Khanna D, Kurzyna M, et al. Definitions and diagnosis of pulmonary hypertension. J Am Coll Cardiol. 2013;62(25 Suppl):D42–50.

2 Galie N, Humbert M, Vachiery JL, Gibbs S, Lang I, Torbicki A, et al. 2015 ESC/ERS Guidelines for the diagnosis and treatment of pulmonary hypertension: The Joint Task Force for the Diagnosis and Treatment of Pulmonary Hypertension of the European Society of Cardiology (ESC) and the European Respiratory Society (ERS): Endorsed by: Association for European Paediatric and Congenital Cardiology (AEPC), International Society for Heart and Lung Transplantation (ISHLT). Eur Respir J. 2015;46(4):903–75.

3 Galie N, Rubin L, Hoeper M, Jansa P, Al-Hiti H, Meyer G, et al. Treatment of patients with mildly symptomatic pulmonary arterial hypertension with bosentan (EARLY study): a double-blind, randomised controlled trial. Lancet. 2008;371(9630):2093–100.

4 Humbert M, Sitbon O, Chaouat A, Bertocchi M, Habib G, Gressin V, et al. Pulmonary arterial hypertension in France: results from a national registry. Am J Respir Crit Care Med. 2006;173(9):1023–30.

5 Lador F, Herve P. A practical approach of pulmonary hypertension in the elderly. Semin Respir Crit Care Med. 2013;34(5):654–64.

6 Berger RM, Beghetti M, Humpl T, Raskob GE, Ivy DD, Jing ZC, et al. Clinical features of paediatric pulmonary hypertension: a registry study. Lancet. 2012;379(9815):537–46.

7 Rich JD, Archer SL, Rich S. Noninvasive cardiac output measurements in patients with pulmonary hypertension. Eur Respir J 2013;42(1):125–33.

8 Lador F, Herve P, Bringard A, Gunther S, Garcia G, Savale L, et al. Non-Invasive Determination of Cardiac Output in Pre-Capillary Pulmonary Hypertension. PloS one 2015;10(7):e0134221.

9 Swift AJ, Rajaram S, Hurdman J, Hill C, Davies C, Sproson TW, et al. Noninvasive estimation of PA pressure, flow, and resistance with CMR imaging: derivation and prospective validation study from the ASPIRE registry. JACC Cardiovasc Imag. 2013;6(10):1036–47.

10 Garcia-Alvarez A, Fernandez-Friera L, Mirelis JG, Sawit S, Nair A, Kallman J, et al. Non-invasive estimation of pulmonary vascular resistance with cardiac magnetic resonance. Eur Heart J. 2011;32(19):2438–45.

11 Lau EM, Vanderpool RR, Choudhary P, Simmons LR, Corte TJ, Argiento P, et al. Dobutamine stress echocardiography for the assessment of pressure-flow relationships of the pulmonary circulation. Chest. 2014;146(4):959–66.

12 Swift AJ, Rajaram S, Marshall H, Condliffe R, Capener D, Hill C, et al. Black blood MRI has diagnostic and prognostic value in the assessment of patients with pulmonary hypertension. Eur Radiol. 2012;22(3):695–702.

13 Ameli-Renani S, Ramsay L, Bacon JL, Rahman F, Nair A, Smith V, et al. Dual-energy computed tomography in the assessment of vascular and parenchymal enhancement in suspected pulmonary hypertension. J Thorac Imaging. 2014;29(2):98–106.

14 Ameli-Renani S, Rahman F, Nair A, Ramsay L, Bacon JL, Weller A, et al. Dual-energy CT for imaging of pulmonary hypertension: challenges and opportunities. Radiographics. 2014;34(7):1769–90.

15 Karcaaltincaba M, Aktas A. Dual-energy CT revisited with multidetector CT: review of principles and clinical applications. Diagn Interv Radiol. 2011;17(3):181–94.

16 Primak AN, Ramirez Giraldo JC, Liu X, Yu L, McCollough CH. Improved dual-energy material discrimination for dual-source CT by means of additional spectral filtration. Med Phys. 2009;36(4):1359–69.

17 Fornaro J, Leschka S, Hibbeln D, Butler A, Anderson N, Pache G, et al. Dual- and multi-energy CT: approach to functional imaging. Insights Imaging. 2011;2(2):149–59.

18 Johnson TR, Krauss B, Sedlmair M, Grasruck M, Bruder H, Morhard D, et al. Material differentiation by dual energy CT: initial experience. Eur Radiol. 2007;17(6):1510–7.

19 Thieme SF, Johnson TR, Reiser MF, Nikolaou K. Dual-energy lung perfusion computed tomography: a novel pulmonary functional imaging method. Semin Ultrasound CT MR. 2010;31(4):301–8.

20 Mettler FA, Jr., Huda W, Yoshizumi TT, Mahesh M. Effective doses in radiology and diagnostic nuclear medicine: a catalog. Radiology. 2008;248(1):254–63.

21 Zhang LJ, Yang GF, Zhao YE, Zhou CS, Lu GM. Detection of pulmonary embolism using dual-energy computed tomography and correlation with cardiovascular measurements: a preliminary study. Acta Radiol. 2009;50(8):892–901.

22 Schenzle JC, Sommer WH, Neumaier K, Michalski G, Lechel U, Nikolaou K, et al. Dual energy CT of the chest: how about the dose? Invest Radiol. 2010;45(6):347–53.

23 Ko JP, Brandman S, Stember J, Naidich DP. Dual-energy computed tomography: concepts, performance, and thoracic applications. J Thoracic Imaging. 2012;27(1):7–22.

24 Boroto K, Remy-Jardin M, Flohr T, Faivre JB, Pansini V, Tacelli N, et al. Thoracic applications of dual-source CT technology. Eur J Radiol. 2008;68(3):375–84.

25 Pontana F, Faivre JB, Remy-Jardin M, Flohr T, Schmidt B, Tacelli N, et al. Lung perfusion with dual-energy multidetector-row CT (MDCT): feasibility for the evaluation of acute pulmonary embolism in 117 consecutive patients. Acad Radiol. 2008;15(12):1494–504.

26 Fink C, Johnson TR, Michaely HJ, Morhard D, Becker C, Reiser M, Nikolaou K. Dual-energy CT angiography of the lung in patients with suspected pulmonary embolism: initial results. RoFo. 2008;180(10):879–83.

27 Sueyoshi E, Tsutsui S, Hayashida T, Ashizawa K, Sakamoto I, Uetani M. Quantification of lung perfusion blood volume (lung PBV) by dual-energy CT in patients with and without pulmonary embolism: preliminary results. Eur J Radiol. 2011;80(3):e505–509.

28 Ferda J, Ferdova E, Mirka H, Baxa J, Bednarova A, Flohr T, et al. Pulmonary imaging using dual-energy CT, a role of the assessment of iodine and air distribution. Eur J Radiol. 2011;77(2):287–93.

29 Chae EJ, Seo JB, Jang YM, Krauss B, Lee CW, Lee HJ, Song KS. Dual-energy CT for assessment of the severity of acute pulmonary embolism: pulmonary perfusion defect score compared with CT angiographic obstruction score and right ventricular/left ventricular diameter ratio. AJR Am J Roentgenol. 2010;194(3):604–10.

30 Thieme SF, Ashoori N, Bamberg F, Sommer WH, Johnson TR, Leuchte H, et al. Severity assessment of pulmonary embolism using dual energy CT – correlation of a pulmonary perfusion defect score with clinical and morphological parameters of blood oxygenation and right ventricular failure. Eur Radiol. 2012;22(2):269–78.

31 Bauer RW, Frellesen C, Renker M, Schell B, Lehnert T, Ackermann H, et al. Dual energy CT pulmonary blood volume assessment in acute pulmonary embolism – correlation with D-dimer level, right heart strain and clinical outcome. Eur Radiol. 2011;21(9):1914–21.

32 Kang MJ, Park CM, Lee CH, Goo JM, Lee HJ. Focal iodine defects on color-coded iodine perfusion maps of dual-energy pulmonary CT angiography images: a potential diagnostic pitfall. AJR Am J Roentgenol. 2010;195(5):W325–30.

33 Hoey ET, Agrawal SK, Ganesh V, Gopalan D, Screaton NJ. Dual energy CT pulmonary angiography: findings in a patient with chronic thromboembolic pulmonary hypertension. Thorax. 2009;64(11):1012.

34 Nakazawa T, Watanabe Y, Hori Y, Kiso K, Higashi M, Itoh T, Naito H. Lung perfused blood volume images with dual-energy computed tomography for chronic thromboembolic pulmonary hypertension: correlation to scintigraphy with single-photon emission computed tomography. J Comput Assist Tomogr. 2011;35(5):590–5.

35 Renard B, Remy-Jardin M, Santangelo T, Faivre JB, Tacelli N, Remy J, Duhamel A. Dual-energy CT angiography of chronic thromboembolic disease: can it help recognize links between the severity of pulmonary arterial obstruction and perfusion defects? Eur J Radiol. 2011;79(3):467–72.

36 Hoey ET, Mirsadraee S, Pepke-Zaba J, Jenkins DP, Gopalan D, Screaton NJ. Dual-energy CT angiography for assessment of regional pulmonary perfusion in patients with chronic thromboembolic pulmonary hypertension: initial experience. AJR Am J Roentgenol. 2011;196(3):524–32.

37 Soler X, Kerr KM, Marsh JJ, Renner JW, Hoh CK, Test VJ, Morris TA. Pilot study comparing SPECT perfusion scintigraphy with CT pulmonary angiography in chronic thromboembolic pulmonary hypertension. Respirology. 2012;17(1):180–4.

38 Castaner E, Gallardo X, Ballesteros E, Andreu M, Pallardo Y, Mata JM, Riera L. CT diagnosis of chronic pulmonary thromboembolism. Radiographics. 2009;29(1):31–50; discussion 50–53.

39 Pitton MB, Kemmerich G, Herber S, Schweden F, Mayer E, Thelen M. Chronic thromboembolic pulmonary hypertension: diagnostic impact of Multislice-CT and selective Pulmonary-DSA. RoFo. 2002;174(4):474–9.

40 Tunariu N, Gibbs SJ, Win Z, Gin-Sing W, Graham A, Gishen P, Al-Nahhas A. Ventilation-perfusion scintigraphy is more sensitive than multidetector CTPA in detecting chronic thromboembolic pulmonary disease as a treatable cause of pulmonary hypertension. J Nucl Med. 2007;48(5):680–4.

41 Thieme SF, Graute V, Nikolaou K, Maxien D, Reiser MF, Hacker M, Johnson TR. Dual Energy CT lung perfusion imaging--correlation with SPECT/CT. Eur J Radiol. 2012;81(2):360–5.

42 Lisbona R, Kreisman H, Novales-Diaz J, Derbekyan V. Perfusion lung scanning: differentiation of primary from thromboembolic pulmonary hypertension. AJR Am J Roentgenol. 1985;144(1):27–30.

43 Talwar A, Sarkar P, Patel N, Shah R, Babchyck B, Palestro CJ. Correlation of a scintigraphic pulmonary perfusion index with hemodynamic parameters in patients with pulmonary arterial hypertension. J Thorac Imaging. 2010;25(4):320–5.

44 Pontana F, Remy-Jardin M, Duhamel A, Faivre JB, Wallaert B, Remy J. Lung perfusion with dual-energy multi-detector row CT: can it help recognize ground glass opacities of vascular origin? Acad Radiol. 2010;17(5):587–94.

45 Lee CW, Seo JB, Lee Y, Chae EJ, Kim N, Lee HJ, et al. A pilot trial on pulmonary emphysema quantification and perfusion mapping in a single-step using contrast-enhanced dual-energy computed tomography. Invest Radiol. 2012;47(1):92–7.

46 Chae EJ, Seo JB, Goo HW, Kim N, Song KS, Lee SD, et al. Xenon ventilation CT with a dual-energy technique of dual-source CT: initial experience. Radiology. 2008;248(2):615–24.

47 Park EA, Goo JM, Park SJ, Lee HJ, Lee CH, Park CM, et al. Chronic obstructive pulmonary disease: quantitative and visual ventilation pattern analysis at xenon ventilation CT performed by using a dual-energy technique. Radiology. 2010;256(3):985–97.

48 Chae EJ, Seo JB, Lee J, Kim N, Goo HW, Lee HJ, et al. Xenon ventilation imaging using dual-energy computed tomography in asthmatics: initial experience. Invest Radiol. 2010;45(6):354–61.

49 Hachulla AL, Pontana F, Wemeau-Stervinou L, Khung S, Faivre JB, Wallaert B, et al. Krypton ventilation imaging using dual-energy CT in chronic obstructive pulmonary disease patients: initial experience. Radiology. 2012;263(1):253–9.

50 Thieme SF, Hoegl S, Nikolaou K, Fisahn J, Irlbeck M, Maxien D, et al. Pulmonary ventilation and perfusion imaging with dual-energy CT. Eur Radiol. 2010;20(12):2882–9.

51 Au VW, Jones DN, Slavotinek JP. Pulmonary hypertension secondary to left-sided heart disease: a cause for ventilation-perfusion mismatch mimicking pulmonary embolism. Br J Radiol. 2001:74(877):86–8.

52 Ruzsics B, Lee H, Zwerner PL, Gebregziabher M, Costello P, Schoepf UJ. Dual-energy CT of the heart for diagnosing coronary artery stenosis and myocardial ischemia-initial experience. Eur Radiol. 2008;18(11):2414–24.

53 Ko SM, Choi JW, Song MG, Shin JK, Chee HK, Chung HW, Kim DH. Myocardial perfusion imaging using adenosine-induced stress dual-energy computed tomography of the heart: comparison with cardiac magnetic resonance imaging and conventional coronary angiography. Eur Radiol. 2011;21(1):26–35.

54 Schwarz F, Ruzsics B, Schoepf UJ, Bastarrika G, Chiaramida SA, Abro JA, et al. Dual-energy CT of the heart--principles and protocols. Eur J Radiol. 2008;68(3):423–33.

55 Ko SM, Song MG, Chee HK, Hwang HK, Feuchtner GM, Min JK. Diagnostic performance of dual-energy CT stress myocardial perfusion imaging: direct comparison with cardiovascular MRI. AJR Am J Roentgenol. 2014;203(6):W605–613.

56 Bauer RW, Kerl JM, Fischer N, Burkhard T, Larson MC, Ackermann H, Vogl TJ. Dual-energy CT for the assessment of chronic myocardial infarction in patients with chronic coronary artery disease: comparison with 3-T MRI. AJR Am J Roentgenol. 2010;195(3):639–46.

57 Wichmann JL, Bauer RW, Doss M, Stock W, Lehnert T, Bodelle B, et al. Diagnostic accuracy of late iodine-enhancement dual-energy computed tomography for the detection of chronic myocardial infarction compared with late gadolinium-enhancement 3-T magnetic resonance imaging. Invest Radiol. 2013;48(12):851–6.

Figures (large format)

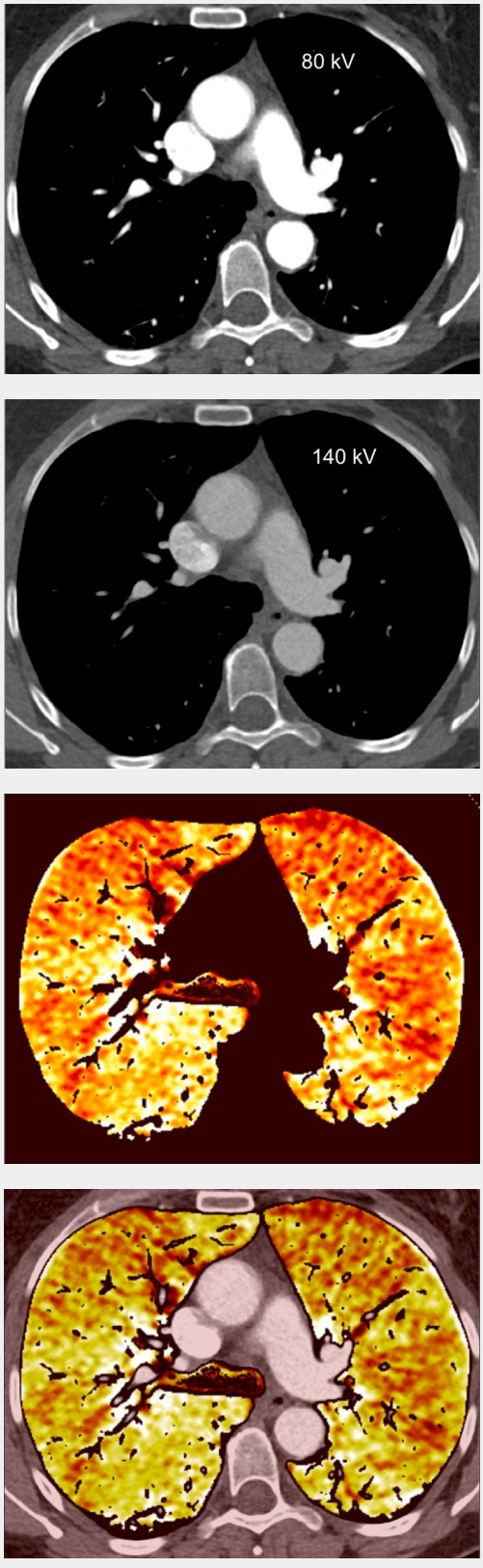

Figure 1

Technical principles. The dual-energy system with two X-ray tubes permits simultaneous 80 (**A**) and 140 kV (**B**) image acquisition in order to generate an iodine map (**C**) fused with mediastinal reconstructions (**D**).

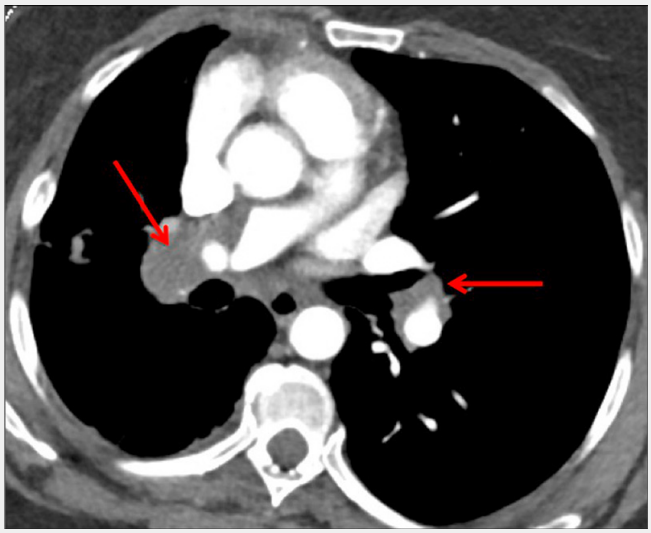

A

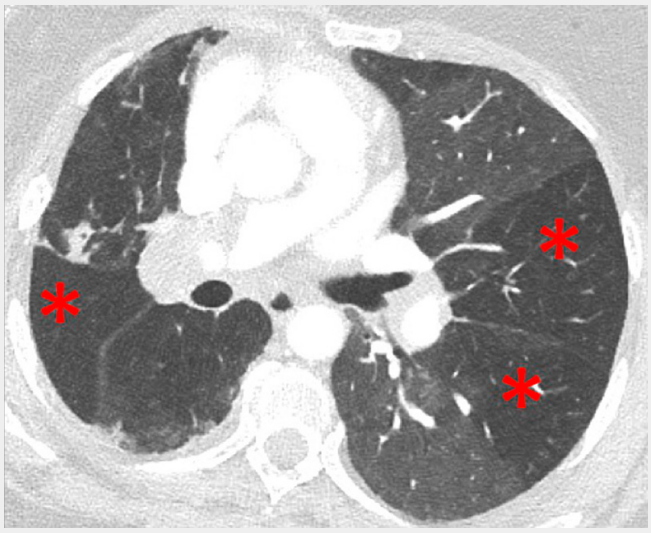

B

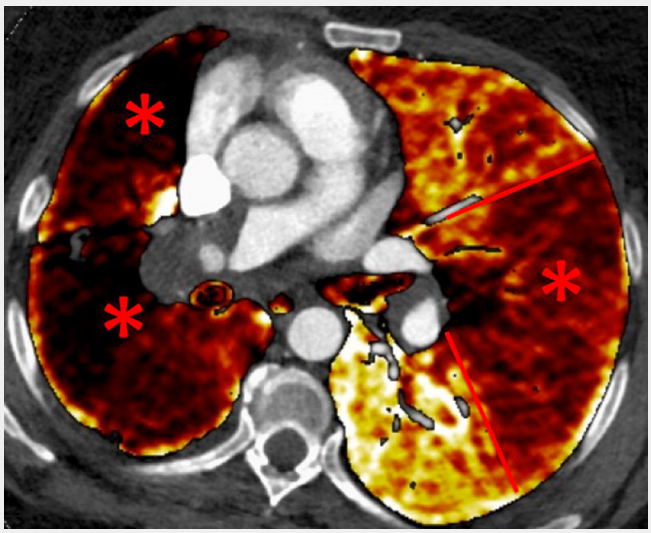

C

Figure 2

Chronic thromboembolic pulmonary hypertension (CTEPH). Vascular (**A**) and parenchymal (**B**) signs of CTEPH with proximal marginal occlusion (arrows) and mosaic pattern (stars). Functional information simply added with triangular perfusion defects (stars) on the iodine maps (**C**).

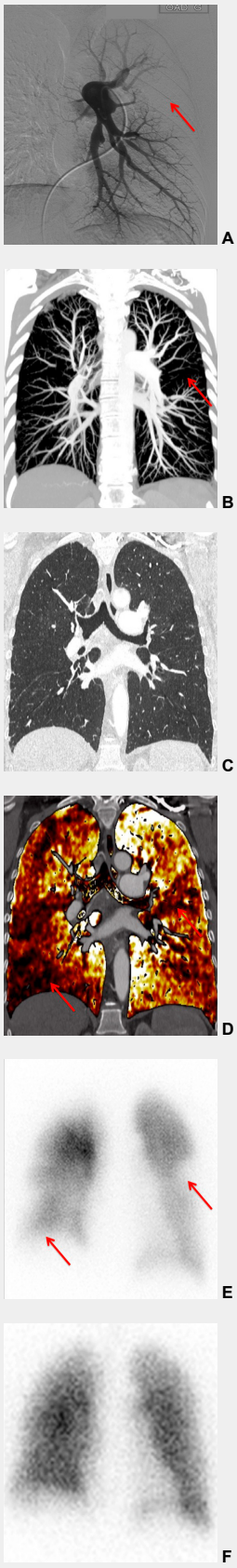

Figure 3

Chronic thromboembolic pulmonary hypertension (CTEPH). Segmental occlusions of pulmonary arteries (arrow) in the pulmonary angiography (**A**) are clearly visible on the CT angiography (**B**), with normal lung (**C**), and responsible for triangular perfusion defects (arrows) on the perfusion maps (**D**) confirmed by the ventilation-perfusion scintigraphy (**E–F**).

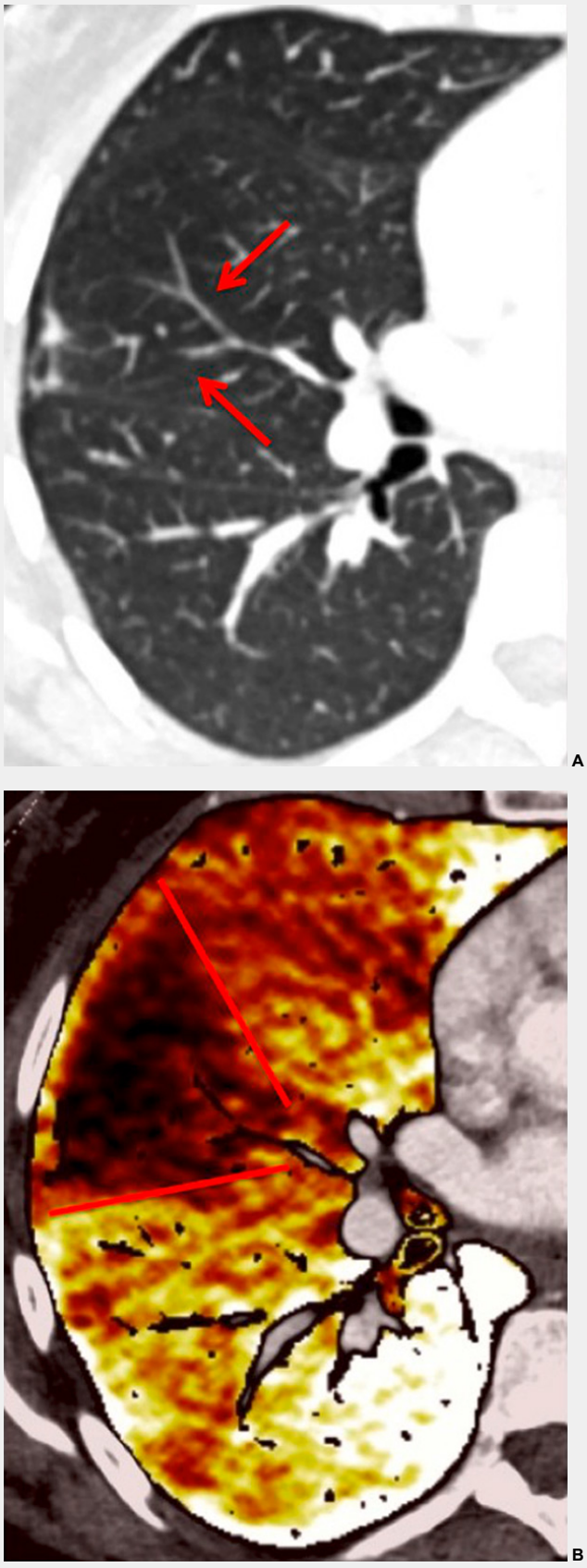

Figure 4

Peripheral chronic thromboembolic pulmonary hypertension (CTEPH). No visible pulmonary artery emboli on standard CTPA are seen (arrows) (**A**) but a wide perfusion defect on the perfusion maps is depicted (**B**) and allows the diagnosis of peripheral CTEPH.

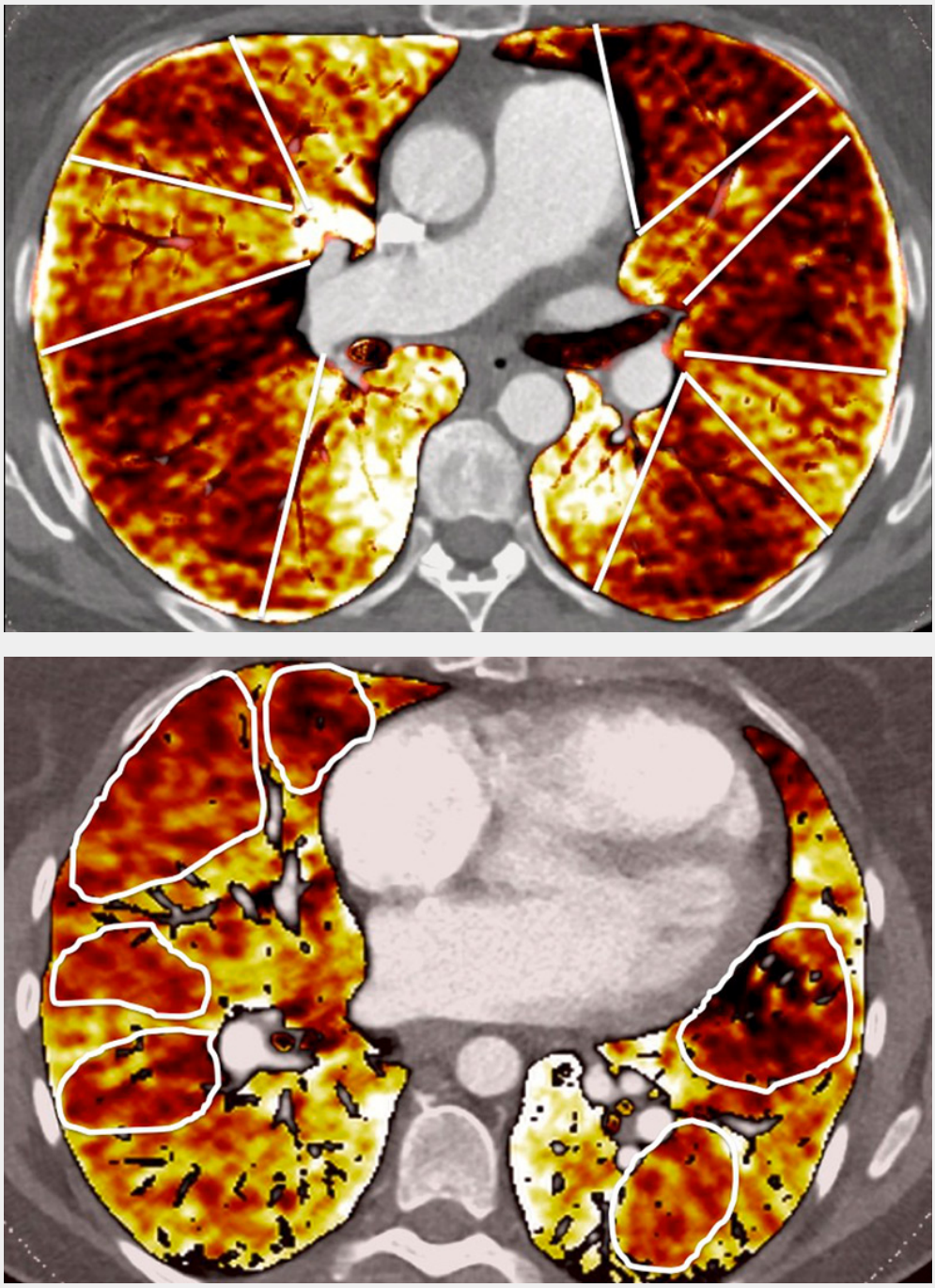

Figure 5

Difference of perfusion defects in pulmonary hypertension depending on the aetiology: triangular well-defined defect seen in chronic thromboembolic pulmonary hypertension (**A**) and poorly defined defect with mottled pattern seen in idiopathic pulmonary arterial hypertension (**B**).

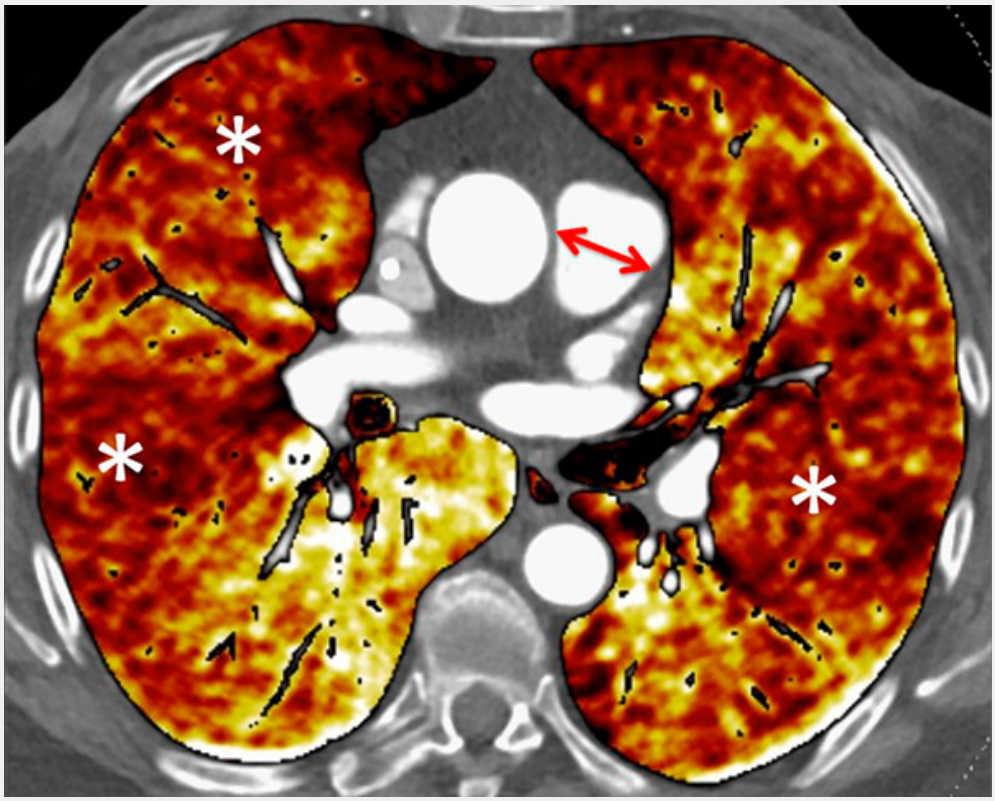

A

B

Figure 6

Perfusion heterogeneities in idiopathic pulmonary artery hypertension (stars) in two different patients (**A/B**). The dilatation of the arteries in pulmonary hypertension (arrows) is not always observed depending on the severity of pulmonary hypertension.

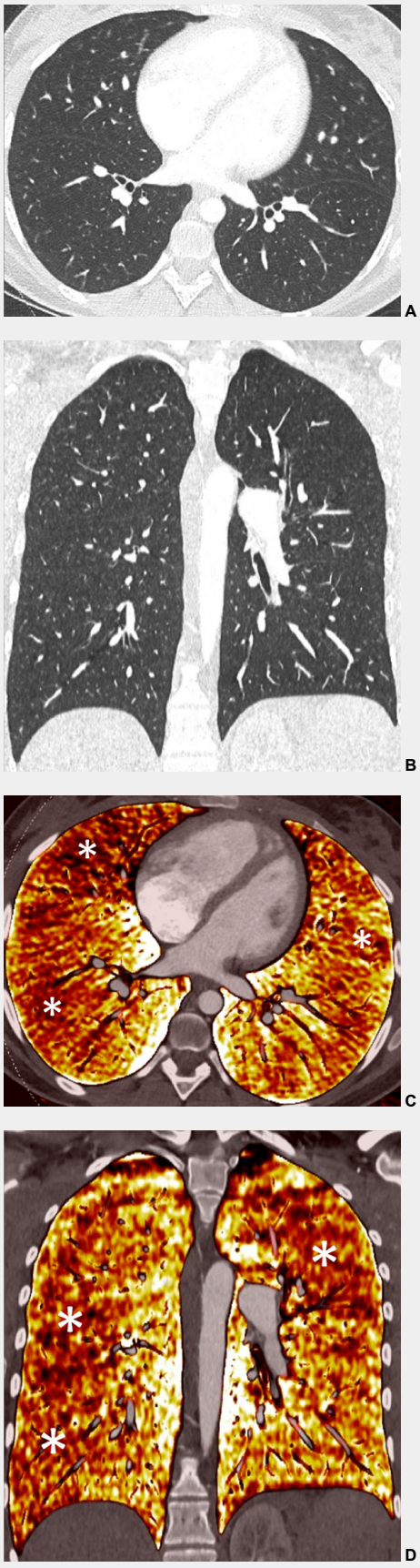

Figure 7

Portopulmonary hypertension in a 16-year-old. No abnormalities were found on morphological computed tomography (**A/B**), but heterogeneous perfusions were present on the perfusion map (stars, **C/D**).

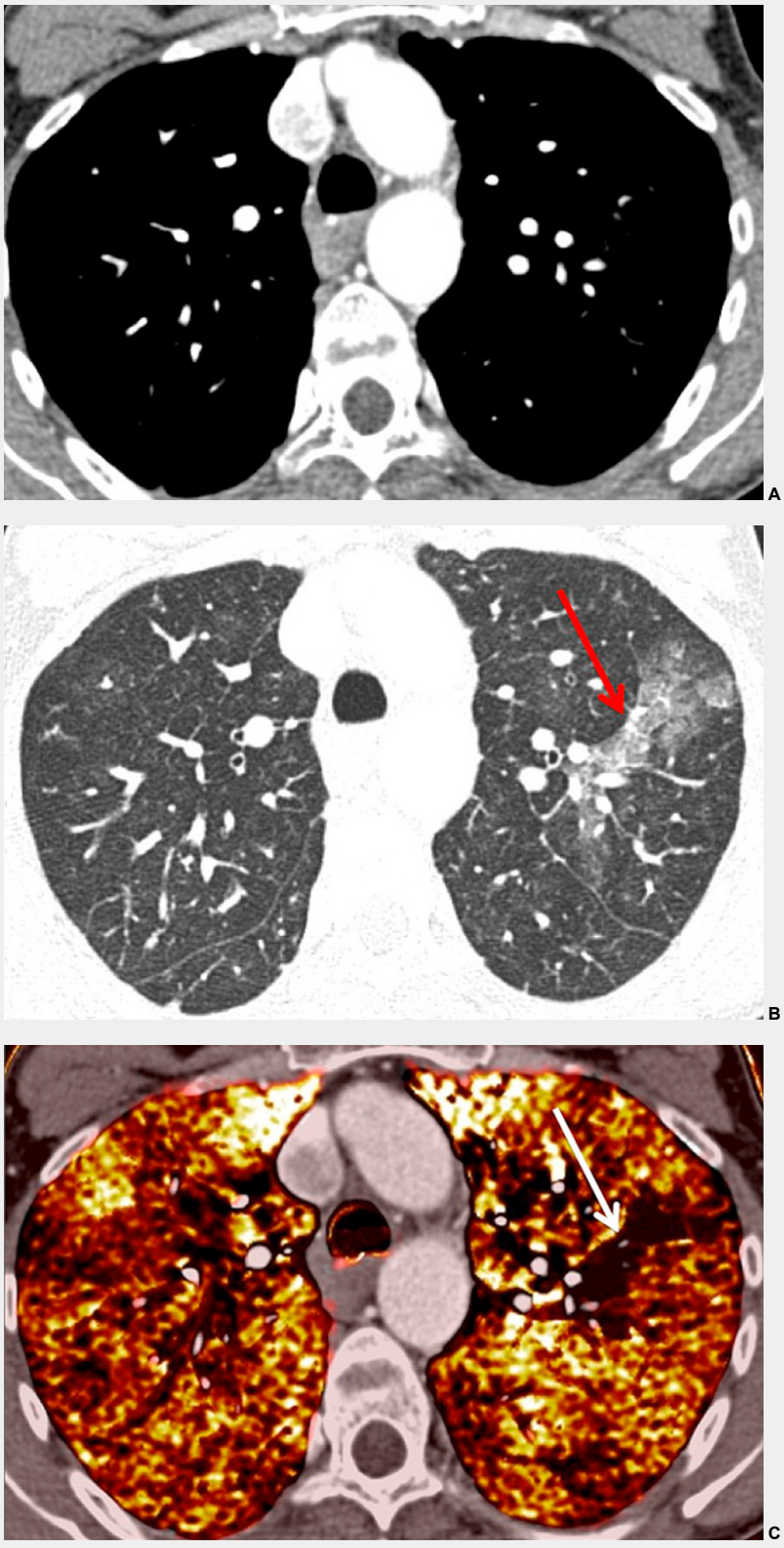

Figure 8

Eisenmenger's syndrome secondary to a large ventricular septal defect. No vascular abnormalities were seen (**A**) but some ground-glass opacities (arrow) (**B**) with the absence of perfusion corresponded to vascular ground-glass opacities surrounded by clear heterogeneous pulmonary perfusion (**C**).

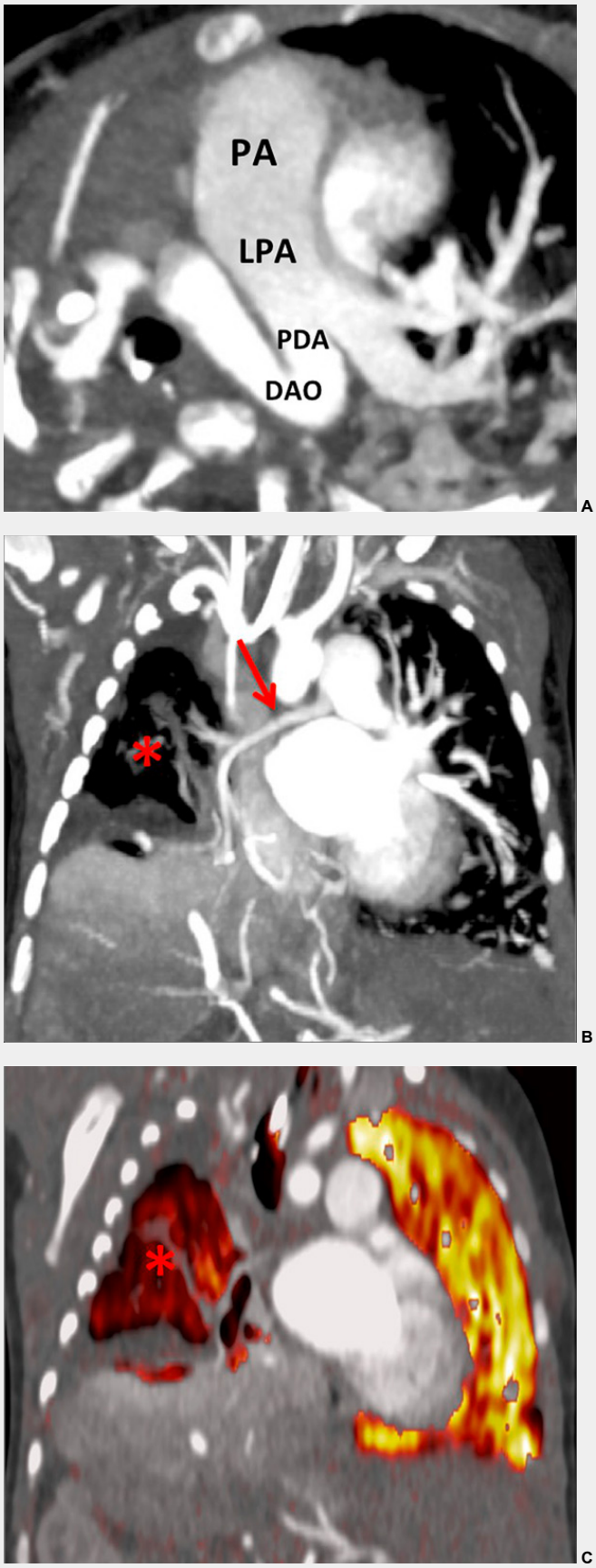

Figure 9

Pulmonary hypertension due to a patent ductus arteriosus (PDA) connecting the descending aorta (DAO) to the left pulmonary artery (LPA) (**A**) in a 2-month-old boy treated for a right diaphragmatic hernia (**B**) resulting in hypoplasia of the right pulmonary artery (arrow). The functional consequences (**C**) are extended hypoperfusion of the right lung (star).

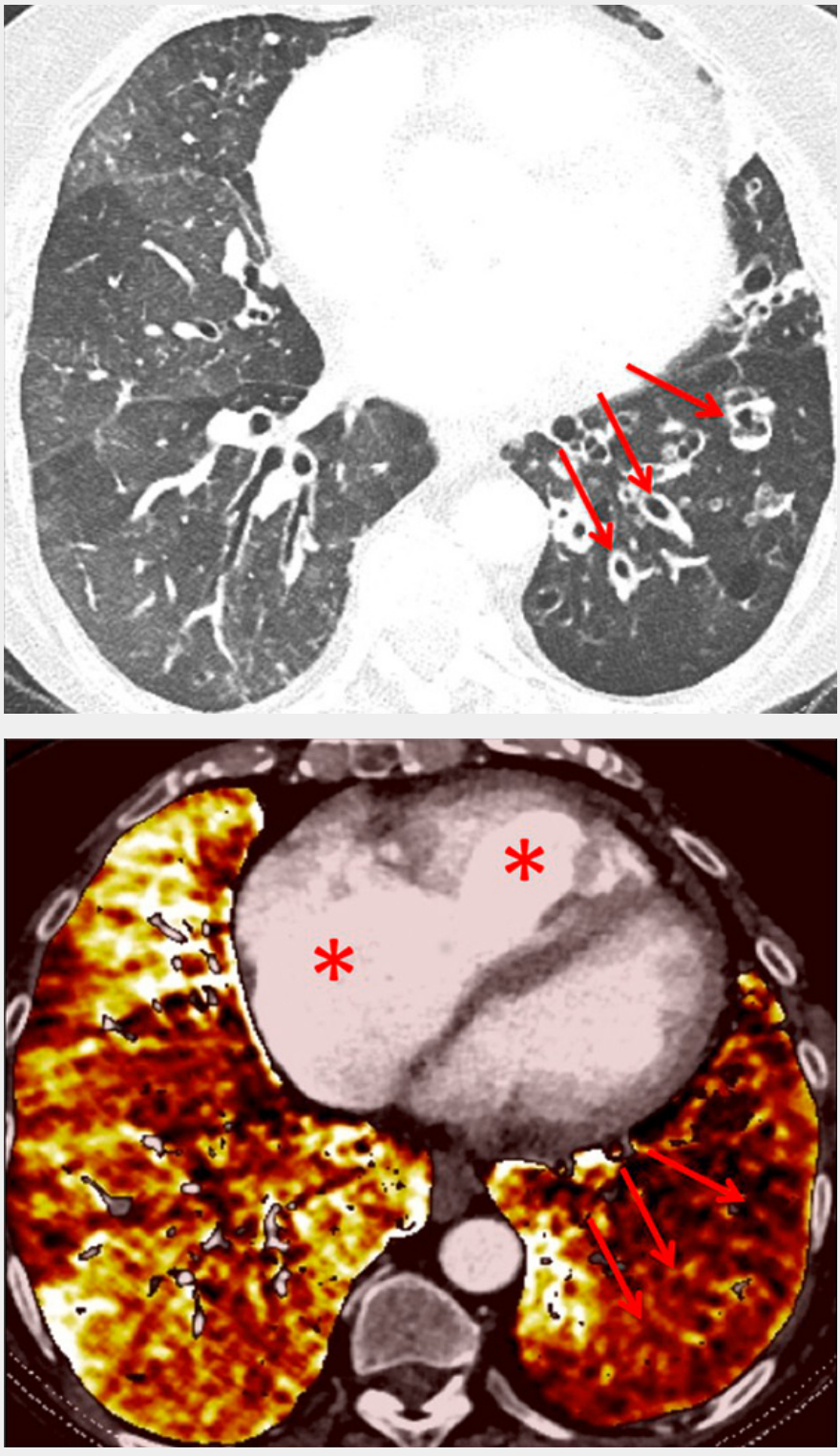

Figure 10

Severe bronchopathy (arrow) in the left lower lobe (**A**) associated with extended hypoperfusion (arrow) and dilatation of the right cardiac cavities (stars) (**B**).

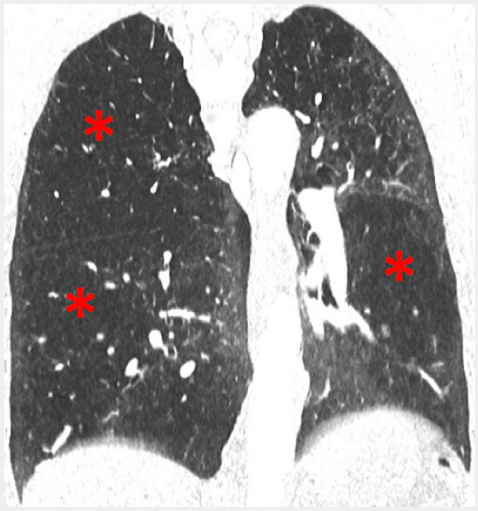

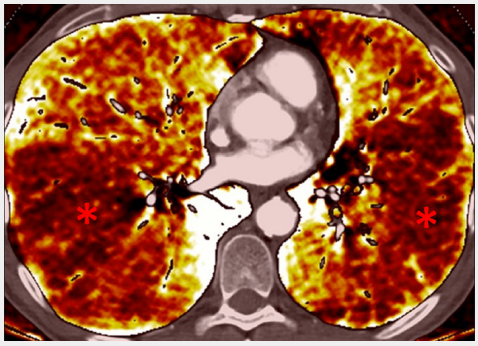

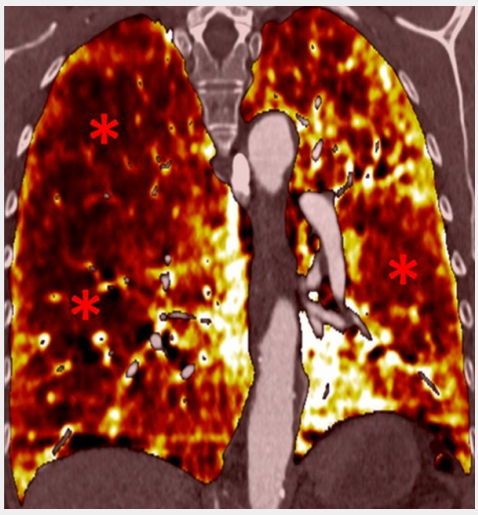

Figure 11

Chronic obstructive pulmonary disease. Correlation between panlobular emphysema (**A/B**) and pulmonary hypoperfusion (**C/D**) (stars).